Antiphase dynamics of multimode intracavity second-harmonic generation

Wang Jingyi and Paul Mandel
Université Libre de Bruxelles, Campus Plaine, Code Postal 231, 1050 Bruxelles, Belgium
(Received 8 March 1993)

We study analytically the properties of second-harmonic generation in a laser cavity. We determine the general criterion of stability for stable steady-state multimode operation. When this condition is not verified we construct analytically the emerging periodic solutions and show that they display antiphase dynamics. When the steady state is stable, we prove that there are four internal frequencies irrespective of the mode number. We show that in this case antiphase dynamics occurs in the transient relaxation to the stable steady state and in the response to noise. Transient antiphase dynamics is shown to imply the disappearance of low-frequency features in the total intensity whose power and noise spectra display a single maximum.

PACS number(s): 42.60.Mi, 42.60.Lh, 42.55.Rz

I. INTRODUCTION

The purpose of this paper is to study analytically the antiphase dynamics that occurs in multimode lasers with intracavity frequency-doubling crystals. Antiphase states were first reported as such by Hadley and Beasly [1] in their study of Josephson junctions. Similar states were then identified in more formal models [2]. Initially, antiphase dynamics was defined as a property of multimode systems (optical or not) in which all modes are in the same periodic state, each mode being shifted from the previous mode by $1/N$ of the period if N is the mode number. This dynamics was found experimentally [3] in the output of a diode-pumped laser with intracavity doubling crystal. A similar dynamics was predicted by Otsuka [4] for deeply modulated multimode Fabry-Pérot lasers; he also investigated its consequence for signal processing. It was progressively realized that the mathematical properties that lie behind antiphase dynamics also account for the fact that in the same systems, the total intensity may have a much smoother behavior than the separate modes. This was verified in the chaotic regime [5,6], in the transient relaxation to steady state [7,8] and in the noise spectrum of multimode Fabry-Pérot lasers [9].

Intracavity nonlinear processes were suggested already since the early days of laser physics by Kroll [10]. The early theory of intracavity parametric oscillation (covering both subharmonic and second harmonic generations) was proposed by Oshman and Harris [11]. However, this problem remained mostly academic until Baer [12] succeeded in operating a diode-pumped YAG laser with intracavity doubling crystals in steady state. His numerical modeling showed the importance of sum-frequency generation in the nonlinear crystal as a source to the "green problem", i.e., irregular amplitude fluctuations in the output. This effect was shown by James, Harrell, and Roy [13] to be a manifestation of chaotic dynamics. The next step was the realization by Oka and Kubota [14] that the electric field polarization was an important ingredient to explain the observed results, in particular the occurrence of chaos in some configurations. The final touch in the modeling of the Baer setup was brought by James *et al.* [15] who included in the model the birefringence of both the YAG and the doubling crystal and the angle between the optical fast axes of the two crystals. A review of this modeling has been given recently by Roy, Bracikowski, and James [16]. An alternative model has been proposed by Victorov and coworkers [17,18] in which the spatial grating in the lasing cavity is included (as in the Tang, Statz, and deMars rate equations) but the birefringence and the two directions of polarizations are not taken into account. This model seems to describe adequately the chaotic dynamics and the role of the phase-sensitive interactions in destabilizing the laser.

In this paper, we analyze in a systematic way the rate equations derived by Roy, Bracikowski, and James [16] to find an analytic explanation to the properties displayed by intracavity second-harmonic generation. In particular, our purpose is to understand the origin of the antiphase dynamics in the periodic regime. Although this goal is far too ambitious at present, we shall show that a perturbation analysis leads to information that begins to clarify this type of dynamics. In particular, we shall show that we can construct antiphase states, though their stability is not proved. Their unicity is also an open question to which we do not bring any clarification.

This paper is organized as follows. In Sec. II we recall the model equations and derive the general expression for the linear stability of a steady state consisting of M modes polarized in one direction and P modes polarized in the orthogonal direction (M and P arbitrary). In Sec. III we study the case in which all modes oscillate with the same polarization ($P=0$) and construct analytically, by perturbation, the antiphase solution. In Sec. IV we study the case where an equal number of modes oscillate in each polarization ($M=P$). The main results are derived in Sec. V, where the general case is solved asymptotically, exploiting different scales that are suggested by the experimental data. Here again, we derive the condition of stability for the steady-state operation and construct the

periodic solutions that emerge when the steady state becomes unstable. We show that antiphase states are a subset of the solutions to this problem. Finally, in Sec. VI we study the steady-state regime and characterize it by means of two oscillation frequencies that appear either in the noise spectrum or in the power spectrum associated with the relaxation to the steady state.

II. RATE EQUATIONS AND LINEAR STABILITY

Practically all experiments on intracavity second-harmonic generation have been performed on diode laser-pumped Nd:YAG laser with a frequency-doubling crystal placed inside the lasing cavity. As shown by Roy, Bracikowski, and James [16], the following rate equations account fairly well for the observed phenomena:

$$\tau_c \frac{dI_k}{dt} = \left[G_k - \alpha_k - g\epsilon I_k - 2\epsilon \sum_{j \neq k} \mu_{jk} I_j \right] I_k \ , \tag{1}$$

$$\tau_f \frac{dG_k}{dt} = \gamma_k - (1 + I_k + \beta \sum_{j \neq k} I_j) G_k \ , \tag{2}$$

where τ_c and τ_f are the cavity round-trip time and fluorescence lifetime, respectively, I_k and G_k are, respectively, the intensity and gain associated with the kth longitudinal mode, α_k is the cavity-loss parameter for the kth mode, γ_k is the small signal gain which is related to the pump rate, β_k is the cross-saturation parameter, and g is a geometrical factor whose value depends on the phase delays of the amplifying and doubling crystals and on the angle between the fast axes of these two crystals. The electric-field modes can oscillate in one of two orthogonal polarizations. In Eq. (1), $\mu_{jk} = g$ if modes j and k have the same polarization while $\mu_{jk} = 1 - g$ if the modes have orthogonal polarizations. ϵ is a nonlinear coefficient whose value depends on the properties of the KTP crystal; it describes the conversion efficiency of the fundamental intensity into the doubled intensity. Finally, following Roy, Bracikowski, and James [16], we simplify the rate equations (1) and (2) by assuming that the cavity loss α_k and the small signal gain γ_k are mode independent: $\alpha_k = \alpha$ and $\gamma_k = \gamma$.

By convention, we shall consider that the first M modes are polarized in the x direction and that the last P modes are polarized in the y direction. Because the coefficient μ varies with the polarization, there is in general no solution with all modes having the same intensities. However, there is a class of solutions for which all modes in a given polarization have the same gain and intensity. Let the common steady state be $(I,G) = (I_s, G_s)$ for the first M modes and $(I,G) = (J_s, H_s)$ for the last P modes. The steady-state equations for the first M modes are

$$G_s = \alpha + (2M-1) g\epsilon I_s + 2\epsilon(1-g) P J_s \ , \tag{3}$$

$$\gamma - G_s [1 + I_s + (M-1)\beta I_s + \beta P J_s] = 0 \ , \tag{4}$$

and the steady-state equations for the last P modes are

$$H_s = \alpha + (2P-1) g\epsilon J_s + 2\epsilon(1-g) M I_s \ , \tag{5}$$

$$\gamma - H_s [1 + J_s + (P-1)\beta J_s + \beta M I_s] = 0 \ . \tag{6}$$

A linear stability analysis of this steady state yields an expression for the stability matrix whose determinant is given by

$$\begin{aligned}
\mathcal{D}(\lambda) = (-1)^{M+P} & \left[(\tau_c\lambda - g\epsilon I_s)\left(\tau_f\lambda + \frac{\gamma}{G_s}\right) + (1-\beta) I_s G_s \right]^{M-1} \left[(\tau_c\lambda - g\epsilon J_s)\left(\tau_f\lambda + \frac{\gamma}{H_s}\right) + (1-\beta) J_s H_s \right]^{P-1} \\
\times \Bigg\{ & \left[(\tau_c\lambda + g\epsilon I_s)\left(\tau_f\lambda + \frac{\gamma}{G_s}\right) + I_s G_s \right] \left[(\tau_c\lambda + g\epsilon J_s)\left(\tau_f\lambda + \frac{\gamma}{H_s}\right) + J_s H_s \right] \\
& + (P-1) \left[(\tau_c\lambda + g\epsilon I_s)\left(\tau_f\lambda + \frac{\gamma}{G_s}\right) + I_s G_s \right] \left[2g\epsilon J_s \left(\tau_f\lambda + \frac{\gamma}{H_s}\right) + \beta J_s H_s \right] \\
& + (M-1) \left[(\tau_c\lambda + g\epsilon J_s)\left(\tau_f\lambda + \frac{\gamma}{H_s}\right) + J_s H_s \right] \left[2g\epsilon I_s \left(\tau_f\lambda + \frac{\gamma}{G_s}\right) + \beta I_s G_s \right] \\
& + (M-1)(P-1) \left[2g\epsilon I_s \left(\tau_f\lambda + \frac{\gamma}{G_s}\right) + \beta I_s G_s \right] \left[2g\epsilon J_s \left(\tau_f\lambda + \frac{\gamma}{H_s}\right) + \beta J_s H_s \right] \\
& - MP \left[2(1-g)\epsilon I_s \left(\tau_f\lambda + \frac{\gamma}{G_s}\right) + \beta I_s G_s \right] \left[2(1-g)\epsilon J_s \left(\tau_f\lambda + \frac{\gamma}{H_s}\right) + \beta J_s H_s \right] \Bigg\} \ .
\end{aligned} \tag{7}$$

The steady solutions are stable if the roots of the equation $\mathcal{D}(\lambda) = 0$ have a negative real part; one or more positive real parts implies an instability.

Although expression (7) is quite heavy, its structure is simple: $\mathcal{D}(\lambda) = [R(2,\lambda)]^{M-1} [R'(2,\lambda)]^{P-1} R(4,\lambda)$, where $R(n,\lambda)$ and $R'(n,\lambda)$ are real polynomials of degree n in λ. In particular, this limits the number of oscillation frequencies to four if M and P are arbitrary.

III. $M>1$ AND $P=0$

The first case we can analyze in detail is the regime where all modes oscillate with the same polarization. In that case, the determinant (7) of the general stability matrix assumes the simpler form

$$\mathcal{D}=(-1)^M\left[(\tau_c\lambda-g\epsilon I_s)\left[\tau_f\lambda+\frac{\gamma}{G_s}\right]+(1-\beta)I_sG_s\right]^{M-1}$$
$$\times\left\{(\tau_c\lambda+g\epsilon I_s)\left[\tau_f\lambda+\frac{\gamma}{G_s}\right]+I_sG_s+(M-1)\left[2g\epsilon I_s\left[\tau_f\lambda+\frac{\gamma}{G_s}\right]+\beta I_sG_s\right]\right\}. \tag{8}$$

From the characteristic equation $\mathcal{D}(\lambda)=0$, we can easily deduce that all roots have a negative real part provided the following two conditions are verified:

$$g<\frac{\tau_c}{\tau_f}\frac{\gamma}{\epsilon I_sG_s}=g_1 \tag{9}$$

and

$$g<\frac{1-\beta}{\epsilon}\frac{G_s^2}{\gamma}=g_2\ . \tag{10}$$

Note that if we expand I_s and G_s in powers of ϵ, $I_s=p/[1+(M-1)\beta]+O(\epsilon)$ and $G_s=\gamma/(1+p)+O(\epsilon)$ with $p\equiv(\gamma-\alpha)/\alpha$, Eq. (9) reduces to the result (3a) of James *et al.* [15]. However, this expansion also implies that $G_s=\alpha$, which is a rather crude approximation. Furthermore, the second condition, Eq. (10), was overlooked in Ref. [15]. For the parameter values corresponding to the experiments reported in [15], it can be verified that $g_1<g_2$, so that the omission of condition (10) was of no practical consequence. An important result that also derives from the characteristic equation $\mathcal{D}(\lambda)=0$ is the nature of the instabilities that can develop from the steady state $M>1$, $P=0$. There are two possible mechanisms of destabilization. The first one is a Hopf bifurcation towards periodic solutions. It occurs at the critical intensity

$$I_H=\frac{\tau_c/\tau_f}{g\epsilon-[1+(M-1)\beta]\tau_c/\tau_f}\ , \tag{11}$$

provided the geometrical factor verifies the inequality

$$g>\frac{\tau_c}{\tau_f}\frac{1+(M-1)\beta}{\epsilon}\ . \tag{12}$$

A second instability point can occur. It is a steady bifurcation point at $I_C=[-1+\sqrt{\gamma(1-\beta)/g\epsilon}]/[1+(M-1)\beta]$. However, we can show that for $\beta<1$ and $\epsilon\ll1$, we have $I_C>I_H$ and the emerging steady solution is always unstable. Therefore, we shall not study it. When the inequality (12) is not verified, the steady state (3) and (4) is stable and there is no instability point. Figure 1 displays the dependence of the Hopf bifurcation point on the geometrical factor g.

Although we could not construct completely the periodic solutions that emerge from the Hopf bifurcation point, a number of properties of these solutions can be derived. We first introduce scaled variables

$$D_s=G_s\tau_f/\tau_c,\quad E_s=H_s\tau_f/\tau_c,\quad \gamma_0=\gamma\tau_f/\tau_c\ ,$$
$$\alpha_0=\alpha\tau_f/\tau_c,\quad g_0=g\epsilon\tau_f/\tau_c\ , \tag{13}$$
$$g_1=(1-g)\epsilon\tau_f/\tau_c,\quad \tau=t/\tau_f\ .$$

In the vicinity of the Hopf bifurcation, we seek solutions of Eqs. (1) and (2) of the form

$$I_k(\delta,T,\sigma)=I_H+\delta I_{k1}(T,\sigma)+O(\delta^2)\ ,$$
$$D_k(\delta,T,\sigma)=D_H+\delta D_{k1}(T,\sigma)+O(\delta^2)\ , \tag{14}$$

where the small parameter δ, the fast time T, and the slow time σ are defined by

$$\gamma_0=\gamma_H\pm\delta^2,\quad T=\omega\tau\ ,$$
$$\sigma=\delta^2\tau,\quad \omega^2=I_HD_H(1-\beta)-g_0I_H\gamma_H/D_H\ . \tag{15}$$

In these definitions γ_H is obtained as the solution of the implicit equation $I_H(\gamma)=I_s(\gamma)$. More precisely, we seek $2M$ amplitudes I_k and D_k that are 2π periodic functions of T in the long-time limit $T\to\infty$. An explicit solution of this problem is not available, but the following partial result can be derived. The first-order deviations $I_{k1}(T,\sigma)$ and $D_{k1}(T,\sigma)$ verify the evolution equations

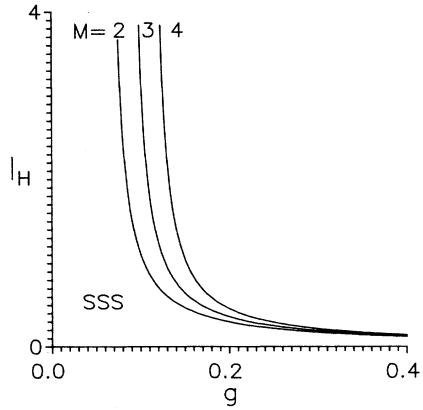

FIG. 1. Dependence of the threshold for destabilization of the steady state in the case where $M>1$ and $P=0$. The steady state is stable below the critical curves. Parameters are $\epsilon=5\times10^{-5}$, $\tau_c/\tau_f=2\times10^{-6}$, and $\beta=0.6$.

$$\omega\frac{\partial I_{k1}}{\partial T}=I_H\left[D_{k1}-g_0I_{k1}-2g_0\sum_{\substack{j=1\\j\neq k}}^{M}I_{j1}\right], \tag{16}$$

$$\omega\frac{\partial D_{k1}}{\partial T}=-\gamma_H D_{k1}/D_H-D_H\left[I_{k1}+\beta\sum_{\substack{j=1\\j\neq k}}^{M}I_{j1}\right]. \tag{17}$$

Let us construct the sum of the first-order corrections to the Hopf intensity and gain: $S_I=\sum_{k=1}^{M}I_{k1}$ and $S_D=\sum_{k=1}^{M}D_{k1}$. From the first-order equations (16) and (17) we obtain for the sum functions the evolution equations

$$\omega\frac{\partial S_D}{\partial T}=-\gamma_H S_D/D_H-D_H S_I[1+\beta(M-1)], \tag{18}$$

$$\frac{\partial^2 S_I}{\partial T^2}+\frac{2Mg_0I_H}{\omega}\frac{\partial S_I}{\partial T}+\frac{I_H}{\omega^2}\{[1+\beta(M-1)]D_H+(2M-1)g_0^2I_H\}S_I=0. \tag{19}$$

From these equations, it follows that in the long-time limit both sums S_I and S_D vanish. Using this property, we can verify that in the long-time limit the equation for I_{k1} reduces to $\partial^2 I_{k1}/\partial T^2+I_{k1}=0$. Therefore, the first-order modal solutions must have the asymptotic form

$$\begin{aligned}I_{j1}&=a_jA(\sigma)e^{iT}+\text{c.c},\\ D_{j1}&=\left[\frac{i\omega}{I_H}-g\epsilon\frac{\tau_f}{\tau_c}\right]a_jA(\sigma)e^{iT}+\text{c.c.},\end{aligned} \tag{20a}$$

with the constraint $\sum_{k=1}^{M}a_k=0$ expressing the fact that S_D and S_I vanish. A nontrivial solution of this constraint equation is

$$a_k=\exp(2\pi ikm/M), \tag{20b}$$

where $k=1,2,\ldots,M$ and $m=0,1,2,\ldots,M-1$. Using the identity

$$\sum_{k=1}^{M}x^k=\frac{x(1-x^M)}{1-x},$$

it is easy to verify with $x=\exp(2\pi im/M)$ that (20b) is a solution of the constraint equation. The solutions (20a) and (20b) form an antiphase state if $m\neq 0$. Indeed, we have in this way a periodic solution in which all modal intensities have the same period and amplitude, each mode being shifted from another by $1/M$ of the period. This is precisely the property associated with antiphase dynamics for periodic solutions [1,2]. Another property of these solutions which is evident from (20b) is the high degree of degeneracy. There are $(M-1)!$ equivalent antiphase states and one in-phase state (associated with $m=0$). A complete analysis of these solutions would require that we construct the amplitudes $A(\sigma)$. This task will not be carried out here because of the amount of algebra involved in this construction which requires the derivation of the solvability condition from the $O(\delta^3)$ equations. Another point that needs elucidation is the behavior of the total intensity. Although we have shown that S_I tends to zero in the long-time limit, this is only a perturbative result. If we analyze numerically Eqs. (1) and (2), we find that the total intensity should be a $2\pi/M$ periodic function, i.e., it should have a dominant contribution of the form $\exp(\pm iMT)$. In the frame of the perturbation expansion (14), such a function cannot appear before the order δ^M. It is therefore consistent that the sum vanishes at order one in δ. It is also clear that the perturbative approach we have used to analyze the modal intensities is not adequate to study the total intensity, for which a global approach is needed. In the case of the laser rate equations, we have been able to describe such an approach [19]. However, we have not been able to apply the same technique here.

IV. $M=P>1$

Another case that can be considered in detail is the equipartition of modes in both directions of polarization. In this case, the symmetry between the two sets of modes suggests that we seek solutions with equal intensity and gain in all modes: $(I_s,G_s)=(J_s,H_s)$. In this case, the characteristic equation that determines the stability factors into two quadratic equations:

$$(\tau_c\lambda-g\epsilon I_s)\left[\tau_f\lambda+\frac{\gamma}{G_s}\right]+(1-\beta)I_sG_s=0, \tag{21}$$

$$\tau_c\tau_f\lambda^2+\left[\tau_c\frac{\gamma}{G_s}+\tau_f\epsilon I_s[(4M-1)g-2M]\right]\lambda+(1-\beta)I_sG_s+\epsilon I_s[(4M-1)g-2M]\frac{\gamma}{G_s}=0. \tag{22}$$

From Eq. (21), we derive the stability conditions

$$g<\frac{\tau_c}{\tau_f}\frac{\gamma}{\epsilon I_sG_s}, \tag{23}$$

$$g<\frac{1-\beta}{\epsilon}\frac{G_s^2}{\gamma}, \tag{24}$$

whereas from Eq. (22) the stability conditions are

$$g>\frac{2M}{4M-1}-\frac{1}{4M-1}\frac{\tau_c}{\tau_f}\frac{\gamma}{\epsilon I_sG_s}, \tag{25}$$

$$g>\frac{2M}{4M-1}-\frac{1}{4M-1}\frac{1-\beta}{\epsilon}\frac{G_s^2}{\gamma}. \tag{26}$$

Here again, an expansion in powers of ϵ gives the results previously obtained by James *et al.* [15], but only with the conditions (23) and (25). Conditions (24) and (26) are missing in [15]. We can combine the stability conditions (23) with (25), and the stability conditions (24) with (26) to get the following inequalities:

$$\frac{\tau_c}{\tau_f}\frac{\gamma}{\epsilon I_sG_s}>\tfrac{1}{2}, \tag{27}$$

$$\frac{1-\beta}{\epsilon}\frac{G_s^2}{\gamma}>\tfrac{1}{2}. \tag{28}$$

Each of the equations (21) and (22) may lead to either a steady bifurcation or to a Hopf bifurcation. They occur at the critical intensities:

$$I_{H1}=\frac{\tau_c/\tau_f}{g\epsilon-[1+(2M-1)\beta]\tau_c/\tau_f}\ , \tag{29}$$

$$I_{H2}=\frac{\tau_c/\tau_f}{\epsilon[2M-(4M-1)g]-[1+(2M-1)\beta]\tau_c/\tau_f}\ , \tag{30}$$

$$I_{C1}=\frac{-1+\sqrt{\gamma(1-\beta)/g\epsilon}}{1+(2M-1)\beta}\ , \tag{31}$$

$$I_{C2}=\frac{-1+\sqrt{\gamma(1-\beta)/\epsilon[2M-(4M-1)g]}}{1+(2M-1)\beta}\ . \tag{32}$$

As in Sec. II, it can be shown that for $\beta<1$ and $\epsilon\ll 1$, the steady-state bifurcations occur for higher intensities than the Hopf bifurcations; therefore, we do not consider them anymore. Figure 2 shows the dependence of the two Hopf bifurcation points on the geometrical factor g. By analyzing the four conditions (29) and (30), the following classification can be obtained:

(1) If $(\tau_c/\tau_f)\{[1+(2M-1)\beta]/\epsilon\}>\frac{1}{2}$, the steady state is stable.

(2) If $(\tau_c/\tau_f)\{[1+(2M-1)\beta]/\epsilon\}<\frac{1}{2}$, there is at least one Hopf bifurcation.

(a) If $g=\frac{1}{2}$, $I_{H1}=I_{H2}$.

(b) If $g<\frac{1}{2}$, the steady state is destabilized at I_{H2}.

(c) If $g>\frac{1}{2}$, the steady state is destabilized at I_{H1}.

When the steady state is destabilized by a Hopf bifurcation, an analysis similar to the analysis presented at the end of Sec. II leads to the conclusion that antiphase states are solution of the bifurcation equations. We shall not present this analysis here since it is a particular case of the analysis of the general case discussed in the next section.

V. M AND P ARBITRARY

In the general case, a complete analysis of the characteristic equation $\mathcal{D}(\lambda)=0$ using expression (7) seems to be out of reach. However, the domain of parameters in which the experiments of Roy and co-workers were made suggest an approximation that leads to analytic results which are in remarkably good agreement with the exact results obtained numerically. To obtain these results, we first note that the complete characteristic equation factors into three polynomials,

$$(\lambda-g_0I_s)\left[\lambda+\frac{\gamma_0}{D_s}\right]+(1-\beta)I_sD_s=0\ , \tag{33}$$

$$(\lambda-g_0J_s)\left[\lambda+\frac{\gamma_0}{E_s}\right]+(1-\beta)J_sE_s=0\ , \tag{34}$$

$$\lambda^4+b\lambda^3+c\lambda^2+d\lambda+e=0\ , \tag{35}$$

in terms of the scaled variables (13). The coefficients of the quartic equation are defined explicitly in the Appendix. In the experiments reported by Roy and co-workers, there are three classes of dimensionless parameters: (a) D_s, E_s, α_0 and γ_0 are large (≥ 5000); (b) I_s, J_s, g_0, and g_1 are $O(1)$; (c) $\epsilon=5.0\times10^{-5}$ and $\tau_c/\tau_f=2.0\times10^{-6}$ are the small parameters. We shall use these natural scales to analyze the roots of the quartic (35). Let us introduce a parameter $K\gg1$ such that D_s, E_s, α_0, and γ_0 are $O(K)$. The simplest choice is $K=D_s$. It is then easy (though lengthy) to verify that $J_s(K)=I_s(K)[1+O(1/K)]$ and $E_s(K)=D_s(K)[1+O(1/K)]$. The four coefficients of the quartic, defined in the Appendix, have the following scaling properties:

$$\begin{aligned} &b=b_0,\quad c=c_1K+c_0\ ,\\ &d=d_1K+d_0,\quad e=e_2K^2+e_1K+e_0\ . \end{aligned} \tag{36}$$

Seeking roots of the quartic (35) in the form $\lambda_{1,2}=u_1\pm iv_1$ and $\lambda_{3,4}=u_2\pm iv_2$, it is easy to verify that $u_k=O(1)$ and $v_k=O(\sqrt{K})$. This leads, to dominant order in K, to the explicit solutions

$$v_1=\{[1+(M+P-1)\beta]I_sD_s\}^{1/2}\ , \tag{37}$$

$$v_2=[(1-\beta)I_sD_s]^{1/2}\ , \tag{38}$$

$$u_1=\frac{-4MPg_1-[M(2M-1)+P(2P-1)]g_0}{2(M+P)}I_s-\frac{\gamma_0}{2D_s}\ , \tag{39}$$

$$u_2=\frac{4MPg_1-[P(2M-1)+M(2P-1)]g_0}{2(M+P)}I_s-\frac{\gamma_0}{2D_s}\ . \tag{40}$$

Although these results are approximations, the corrections are $O(1/K)$ and are fairly small. To verify this point, we have plotted in Fig. 3 the approximate frequencies (37) and (38) and the numerical solution of the stability equations (33)–(35). As expected, the agreement is excellent. The same has been done for the damping rates (39) and (40) compared with the numerical solutions of the stability equations (33)–(35) (Fig. 4). Here again, the agreement is very good. This is quite important since the zeros of u_1 and u_2 will determine the stability domain of the steady state. From these analytic results, it is now easy to derive the general stability condition, which is ob-

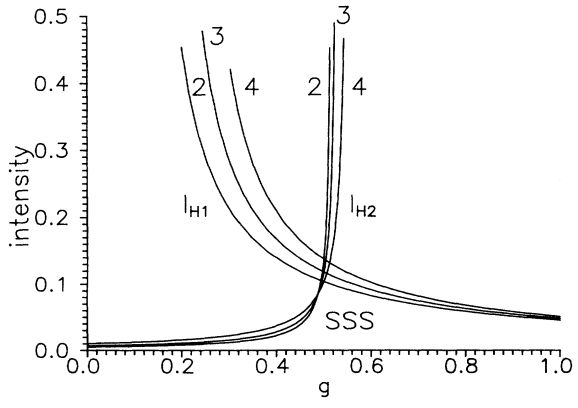

FIG. 2. Dependence of the threshold for destabilization of the steady state in the case where $M=P$. The steady state is stable below both critical curves. Parameters are as in Fig. 1.

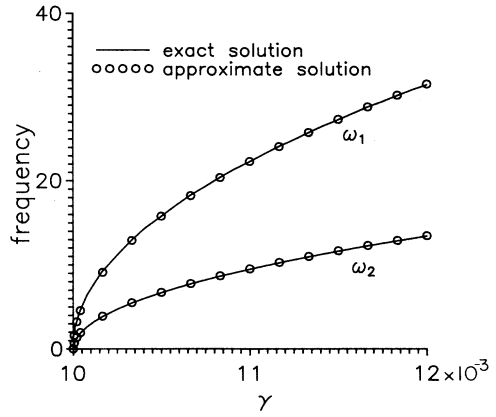

FIG. 3. Frequencies derived from the stability analysis. A comparison between the exact result derived from Eqs. (33)–(35) and the analytic approximation (37) and (38). Parameters are $M=2$, $P=1$, $g=0.52$, and $\alpha=0.01$. The other parameters are as in Fig. 1.

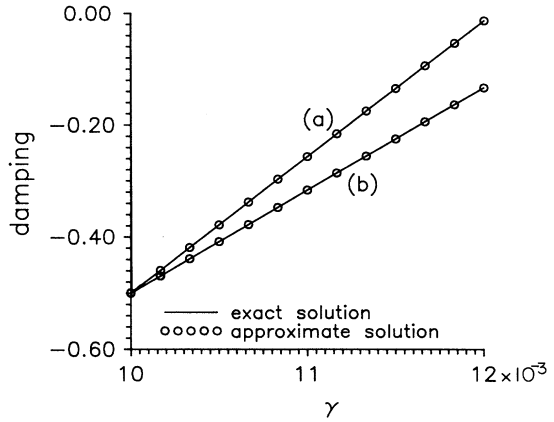

FIG. 4. Damping rates derived from the stability analysis. A comparison between the exact result derived from Eqs. (33)–(35) and the analytic approximation (40). Parameters are as in Fig. 3.

tained by requiring that the real part of all the roots of the quartic and also of the two quadratics (33) and (34) be negative. This leads to

$$g<\frac{\tau_c}{\tau_f}\frac{1}{\epsilon}\frac{\gamma_0}{I_sD_s} \tag{41}$$

and

$$g>\frac{4MP}{(4M-1)P+(4P-1)M}-\frac{M+P}{(4M-1)P+(4P-1)M}\frac{\tau_c}{\tau_f}\frac{1}{\epsilon}\frac{\gamma_0}{I_sD_s}\ . \tag{42}$$

Combining these two inequalities yields the restriction:

$$\frac{\tau_c}{\tau_f}\frac{1}{\epsilon}\frac{\gamma_0}{I_sD_s}>\frac{1}{2} \tag{43}$$

in terms of the variables scaled according to (13). The pair of conditions (41) and (42) represent the general condition of stability for the multimode steady state operation. This steady state operation may be destabilized by Hopf bifurcations leading to periodic solutions. Equations (33) and (34) have both a Hopf bifurcation at the same intensity

$$I_{H1}=\frac{1}{g\epsilon\tau_f/\tau_c-[1+(M+P-1)\beta]}\ . \tag{44}$$

Furthermore, the quartic (35) also has a Hopf bifurcation point at

$$I_{H2}=\frac{1}{\epsilon\left[\frac{4MP}{M+P}-\frac{8MP-M-P}{M+P}g\right]\tau_f/\tau_c-\left[1+(M+P-1)\beta\right]}+O(1/K)\ . \tag{45}$$

The important information is which of the two bifurcation point has the lowest intensity. Analyzing the relations (44) and (45) leads to the following conclusions:

(1) If $(\tau_c/\tau_f)\ \{[1+(M+P-1)\beta]/\epsilon\}>\frac{1}{2}$, there is no instability.

(2) If $(\tau_c/\tau_f)\ \{[1+(M+P-1)\beta]/\epsilon\}<\frac{1}{2}$, there is at least one Hopf bifurcation.

(a) If $g=\frac{1}{2}$, $I_{H1}=I_{H2}$.

(b) If $g<\frac{1}{2}$, the steady state is destabilized at I_{H2}.

(c) if $g>\frac{1}{2}$, the steady state is destabilized at I_{H1}.

Let us now consider the periodic solutions that emerge from the steady state at the first Hopf bifurcation point. In the general case, the evolution equations are

$$\frac{dI_k}{d\tau}=I_k\left[D_k-\alpha_0+g_0I_k-2g_0\sum_{r=1}^{M}I_r-2g_1\sum_{r=1}^{P}J_r\right], \tag{46}$$

$$\frac{dJ_q}{d\tau}=J_q\left[E_q-\alpha_0+g_0J_q-2g_0\sum_{r=1}^{P}J_r-2g_1\sum_{r=1}^{M}I_r\right], \tag{47}$$

$$\frac{dD_k}{d\tau}=\gamma_0-D_k\left[1+(1-\beta)I_k+\beta\sum_{r=1}^{M}I_r+\beta\sum_{r=1}^{P}J_r\right], \tag{48}$$

$$\frac{dE_q}{d\tau}=\gamma_0-E_q\left[1+(1-\beta)J_q+\beta\sum_{r=1}^{P}J_r+\beta\sum_{r=1}^{M}I_r\right], \tag{49}$$

where $k=1,2,\ldots,M$ indexes the modes in one polarization direction while $q=1,2,\ldots,P$ indexes the modes in the orthogonal polarization. As in Sec. III, we seek periodic solutions of Eqs. (46)–(49) that depend on the parameters δ and the times T and σ defined by

$$Z_m(\delta,T,\sigma)=Z_H+\delta Z_{m1}(T,\sigma)+\delta^2 Z_{m2}(T,\sigma)+O(\delta^3),$$
$$\gamma_0=\gamma_H\pm\delta^2,\quad T=\omega\tau,\quad \sigma=\delta^2\tau. \tag{50}$$

In these definitions Z stands for any of the four sets of variables that verify Eqs. (46)–(49). If the first Hopf bifurcation occurs at I_{H1}, the expression for the unperturbed frequency is $\omega^2=I_H D_H(1-\beta)-g_0 I_H\gamma_H/D_H$, which is an exact result. If the first Hopf bifurcation is at I_{H2}, then we use the expansion of the frequency in powers of K given by $\omega^2=I_H D_H(1-\beta)+O(1)$. To first order in δ, we obtain the evolution equations

$$\omega\frac{\partial I_{k1}}{\partial T}=I_H\left[D_{k1}+g_0 I_{k1}-2g_0\sum_{r=1}^{M}I_{r1}-2g_1\sum_{r=1}^{P}J_{r1}\right], \tag{51}$$

$$\omega\frac{\partial J_{q1}}{\partial T}=J_H\left[E_{q1}+g_0 J_{q1}-2g_0\sum_{r=1}^{P}J_{r1}-2g_1\sum_{r=1}^{M}I_{r1}\right], \tag{52}$$

$$\omega\frac{\partial D_{k1}}{\partial T}=-\gamma_H D_{k1}/D_H-D_H\left[(1-\beta)I_{k1}+\beta\sum_{r=1}^{M}I_{r1}+\beta\sum_{r=1}^{P}J_{r1}\right], \tag{53}$$

$$\omega\frac{\partial E_{q1}}{\partial T}=-\gamma_H E_{q1}/E_H-E_H\left[(1-\beta)J_{q1}+\beta\sum_{r=1}^{P}J_{r1}+\beta\sum_{r=1}^{M}I_{r1}\right]. \tag{54}$$

The structure of these equations suggest that we define the four partial sums

$$I=\sum_{r=1}^{M}I_{r1},\quad J=\sum_{r=1}^{P}J_{r1},\quad D=\sum_{r=1}^{M}D_{r1},\quad E=\sum_{r=1}^{P}E_{r1}, \tag{55}$$

and the two total sums $I_1=I+J$, $D_1=D+E$. The total intensity and gain verify the equations

$$\omega\frac{\partial I_1}{\partial T}=I_H[D_1+g_0 I_1-2(g_0 M+g_1 P)I-2(g_1 M+g_0 P)J], \tag{56}$$

$$\omega\frac{\partial D_1}{\partial T}=-\gamma_H D_1/D_H-D_H[1-\beta+(M+P)\beta]I_1. \tag{57}$$

However, because $D_1\gg I_1$, I, and J, we can approximate Eq. (56) by $\omega\partial I_1/\partial T=I_H D_1$. Combining this equation with Eq. (57) leads directly to the result that D_1 and $I_1\propto\exp(-|\eta|T)$ in the limit $T\to\infty$.

Next, we consider the evolution equations for the two functions $I_{kq}=I_{k1}+J_{q1}$ and $D_{kq}=D_{k1}+E_{q1}$. Using Eqs. (51)–(54), we easily get

$$\omega\frac{\partial I_{kq}}{\partial T}=I_H[D_{qk}+g_0 I_{kq}-2(g_0+g_1)I_1], \tag{58}$$

$$\omega\frac{\partial D_{kq}}{\partial T}=-\gamma_H D_{kq}/D_H-D_H[(1-\beta)I_{kq}+2\beta I_1]. \tag{59}$$

In the long-time limit, we neglect I_1 in these equations. This leads to a pair of simple equations whose solution is

$$I_{kq}=a_{kq}A(\sigma)e^{iT}+\text{c.c},$$
$$D_{kq}=(-g_0+i\omega/I_H)a_{kq}A(\sigma)e^{iT}+\text{c.c.}, \tag{60}$$

From this result, it appears that a possible solution for Eqs. (51)–(54) is

$$I_{k1}=a_k A(\sigma)e^{iT}+\text{c.c.},$$
$$J_{q1}=b_q A(\sigma)e^{iT}+\text{c.c.}, \tag{61}$$
$$a_{kq}=a_k+b_q.$$

These solutions can be called antiphase states, since the property $I_1=0$ (in the long-time limit) implies

$$\sum_{k=1}^{M}a_k+\sum_{q=1}^{P}b_q=0, \tag{62}$$

and therefore the coefficients a_k and b_q can be of the form $\exp\{[2\pi im/(M+P)]j\}$, where $j=1,2,\ldots,M+P$ and $m=0,1,2,\ldots,M+P-1$. As in the case $P=0$, these states are highly degenerate except for the in-phase state corresponding to $m=0$.

VI. TRANSIENT DYNAMICS

In the previous sections we have concentrated our analysis on the domain of parameters where the multimode steady state is unstable. However, a self-organized behavior is also possible in the transient relaxation towards a stable multimode steady state. We have already analyzed this kind of behavior in a different context [19], and we want to show that the same dynamics occurs here. In fact, the antiphase dynamics has an extension, and retains its meaning, in the approach to the steady state. As explained just after Eq. (7), there can be at most four frequencies for the damped oscillations characterizing the relaxation of the system towards its steady state. Let ω_1, ω_2, ω_3, and ω_4 be the frequencies associated with Eqs. (37), (33), (34), and (38), respectively. In the limit $K\gg1$, suggested by the experiments and used in Sec. V, there remain only two distinct frequencies:

$$\omega_1\simeq\{[1+(M+P-1)\beta]I_s D_s\}^{1/2}, \tag{63}$$

$$\omega_2\simeq\omega_3\simeq\omega_4\simeq[(1-\beta)I_s D_s]^{1/2}. \tag{64}$$

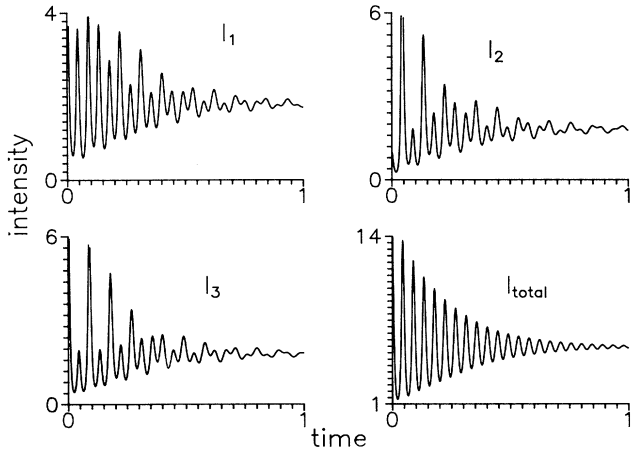

FIG. 5. Transient behavior of the modal intensities with $M=3$ and $P=0$. Parameters are $g=0.9$, $\gamma=0.05$, $\beta=0.6$, $\alpha=0.01$, $\epsilon=10^{-6}$, and $\tau_c/\tau_f=2\times10^{-6}$. Initial condition: $I_1=6$, $I_2=1$, $I_3=8$, $D_1=5015$, $D_2=5010$, $D_3=5005$. The dimensionless time is $\tau=t/\tau_f$ in this and the following figures.

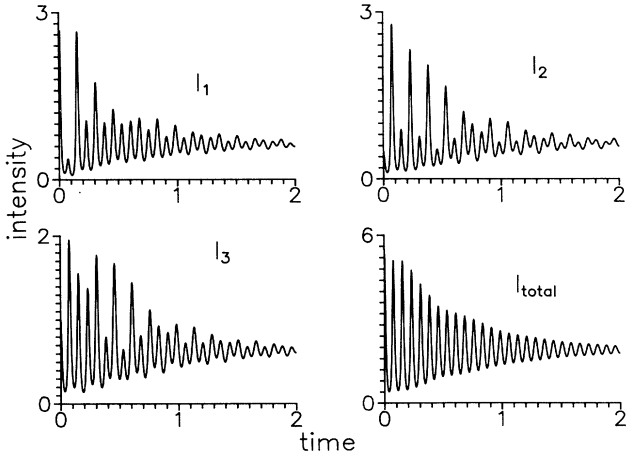

FIG. 7. Transient behavior of the modal intensities with $M=2$ and $P=1$. Parameters are $g=0.9$, $\gamma=0.024$, $\beta=0.6$, $\alpha=0.01$, $\epsilon=10^{-6}$, and $\tau_c/\tau_f=2\times10^{-6}$. Initial condition: $I_1=4$, $I_2=0.5$, $J_1=1$, $D_1=5020$, $D_2=5010$, $E_1=5005$.

Note that these two frequencies cannot be ascribed to specific directions of polarization. However, if we linearize Eqs. (1) and (2) around the steady state, we can easily derive a pair of equations for the total intensity and gain $I=\sum_{k=1}^{M+P}I_k$, $G=\sum_{k=1}^{M+P}G_k$. This pair of equations leads to a *single* damped oscillation frequency which is precisely ω_1 in the same large-K limit. Hence we expect that the total intensity dynamics will be characterized by the single oscillation frequency ω_1, which is the larger of the two frequencies (63) and (64), while each modal intensity (whatever its number) will be characterized by the two frequencies ω_1 and ω_2. This was verified numerically in two ways.

First, we consider the relaxation dynamics. Initially, the system is prepared in an arbitrary state. The transient evolution is recorded for each separate mode and for the total intensity. This is displayed in Fig. 5 for $M=3$ and $P=0$. The antiphase dynamics is quite evident when we compare the modal intensities with the total intensity. In Fig. 6 we display the corresponding power spectra. They confirm the expectation that the total intensity relaxes with a single frequency while the modal intensities relax with two frequencies. For the sake of comparison, Figs. 7 and 8 display the same functions but for a different partition, $M=2$ and $P=1$.

Second, we consider the noise spectrum. If there are only two internal frequencies, they will also characterize the damping of the random fluctuations that naturally occur in the cavity fields. We write formally Eqs. (1) and (2) as $d\,\mathbf{A}/dt=\mathbf{f}(\mathbf{A},\mu)$, where $\mathbf{A}$ is a vector whose components are the modal intensities and gains, while μ stands for all the parameters. Let $\mathbf{B}=\mathbf{B}(\mu)$ be the steady-state solution. We have solved numerically the equation $d\,\mathbf{A}/dt=\mathbf{f}(\mathbf{A},\mu)+0.05\xi(t)\mathbf{B}$, where $\xi(t)$ is a random noise uniformly distributed over the interval $[-1,+1]$ and the initial condition $\mathbf{A}(0)=\mathbf{B}$. This

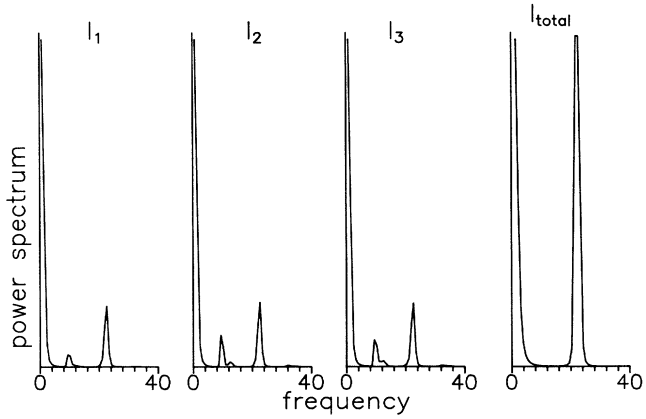

FIG. 6. Power spectrum of the intensities displayed in Fig. 5. Units on the vertical axis are arbitrary but identical for all four spectra.

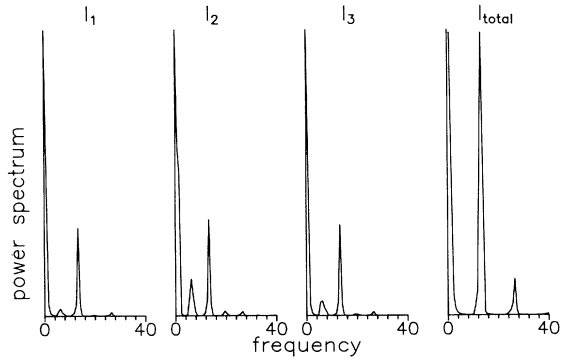

FIG. 8. Power spectrum of the intensities displayed in Fig. 7. Units on the vertical axis are arbitrary but identical for all four spectra.

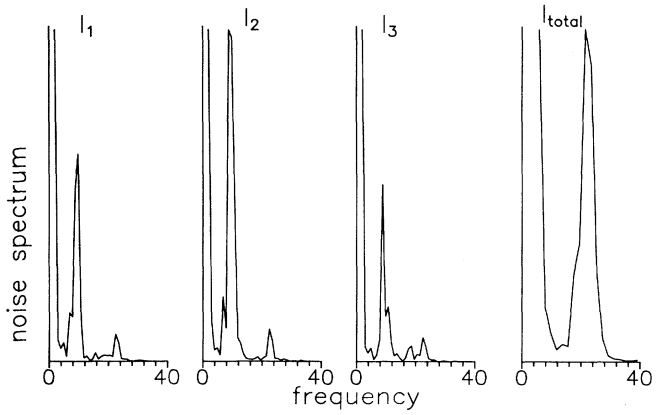

FIG. 9. Noise spectrum in the case where $M=3$ and $P=0$. Same parameters as in Fig. 5.

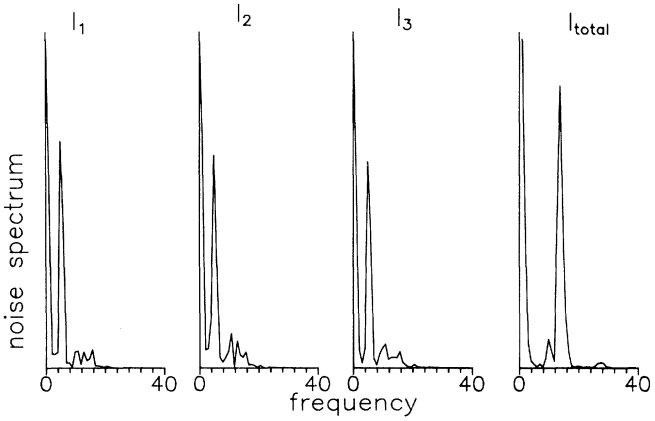

FIG. 10. Noise spectrum in the case where $M=2$ and $P=1$. Same parameters as in Fig. 7.

amounts to starting with the steady state and to adding a noise equal to 5% of the steady-state values. For Figs. 9 and 10 we have taken the same parameters as in Figs. 5 and 7, respectively. Here again, the modal intensities display two peaks (though one of them is usually quite small) while the total intensity displays a single peak at the highest of the two frequencies. In Figs. 9 and 10, it is the peak associated with the lowest frequency that has a large maximum in the modal intensities, while in the relaxation dynamics it is the contrary. This is not a general property and we have verified, e.g., that with four and five modes this rule no longer holds: there is usually a dominant frequency but it can be any of the two internal frequencies.

VII. CONCLUSION

We have shown that it is possible to give an analytic description of the multimode operation of intracavity second-harmonic generation. The salient fact is that the coupling between the active lasing cavity and the doubling crystal induced a new kind of dynamics, the antiphase dynamics, which results from a temporal collective self-organization. This can be traced to the fact that this coupling enables multimode steady solutions to exist. In the domain of stability of the multimode steady state, the antiphase dynamics manifests itself in the transient relaxation dynamics and in the response to noise. In both cases, the total intensity displays a power spectrum with a single peak, while each modal intensity has as many peaks as there are damped oscillation frequencies. When the steady state is not stable, periodic solutions emerge, and we have shown that they display the classic type of antiphase dynamics, i.e., all modes have the same frequency and amplitude, each mode being shifted from another one by a $1/N$ of a period where N is the total number of modes.

A surprising result that we also obtained is the number of damped frequencies. Intuitively, one would expect that number to increase with the number of modes. In fact, for the model of Roy and co-workers it turns out that there are only four internal frequencies, out of which only two can be distinguished in the domain of the parameter where the experiments are conducted: three frequencies differ only by an amount which is $O(1/K)$. A closer look at the determinant (7) indicates that these four frequencies are highly degenerate. Two of them have degeneracy $M-1$ and the other two have degeneracy $P-1$. Thus we recover the expected $M+P$ frequencies.

ACKNOWLEDGMENTS

This research was supported in part by the Fonds National de la Recherche Scientifique and by the Interuniversity Attraction Pole program of the Belgian government. We gratefully acknowledge fruitful discussions with T. Erneux, who clarified for us the discussion of the constraint equation and its solutions (20b).

APPENDIX

The coefficients of the quartic (35) are

$$b=(2M-1)g_0I_s+(2P-1)g_0J_s+\gamma_0(D_s+E_s)/D_sE_s\ ,$$

$$c=(1-\beta+M\beta)I_sD_s+(1-\beta+P\beta)J_sE_s+(2M-1)(2P-1)g_0^2J_sI_s-4MPg_1^2I_sJ_s$$

$$+[(2M-1)I_s+(2P-1)J_s]g_0\gamma_0(D_s+E_s)/D_sE_s+\gamma_0^2/D_sE_s\ ,$$

$$d=(2P-1)[1+(M-1)\beta]g_0I_sJ_sD_s+(2M-1)[1+(P-1)\beta]g_0I_sJ_sE_s$$
$$-2MP\beta g_1I_sJ_s(D_s+E_s)+[1+(M-1)\beta]\gamma_0I_sD_s/E_s+[1+(P-1)\beta]\gamma_0J_sE_s/D_s$$
$$+(2M-1)(2P-1)\gamma_0g_0^2I_sJ_s(D_s+E_s)/D_sE_s-4MP\gamma_0g_1^2I_sJ_s(D_s+E_s)/D_sE_s$$
$$+[(2M-1)I_s+(2P-1)J_s]g_0\gamma_0^2/D_sE_s\ ,$$
$$e=(1-\beta)[1+(M+P-1)\beta]I_sD_sJ_sE_s+(2P-1)[1+(M-1)\beta]g_0\gamma_0I_sJ_sD_s/E_s$$
$$+(2M-1)[1+(P-1)\beta]g_0\gamma_0I_sJ_sE_s/D_s-2MP\beta g_1I_sJ_s\gamma_0(D_s^2+E_s^2)/D_sE_s$$
$$+(2M-1)(2P-1)g_0^2\gamma_0^2I_sJ_s/D_sE_s-4MPg_1^2\gamma_0^2I_sJ_s/D_sE_s\ .$$

[1] P. Hadley and M. R. Beasly, Appl. Phys. Lett. **50**, 621 (1987).

[2] K. Y. Tsang and K. Wiesenfeld, Appl. Phys. Lett. **56**, 495 (1990); K. Wiesenfeld and P. Hadley, Phys. Rev. Lett. **62**, 1335 (1989).

[3] K. Wiesenfeld, C. Bracikowski, G. James, and R. Roy, Phys. Rev. Lett. **65**, 1749 (1990).

[4] K. Otsuka, Phys. Rev. Lett. **67**, 1090 (1991).

[5] C. Bracikowski and R. Roy, Chaos **1**, 49 (1991); Phys. Rev. A **43**, 6455 (1991).

[6] K. Otsuka, P. Mandel, M. Georgiou, and C. Etrich, Jpn. J. Appl. Phys. **32**, L318 (1993).

[7] K. Otsuka, P. Mandel, S. Bielawski, D. Derozier, and P. Glorieux, Phys. Rev. A **46**, 1692 (1992).

[8] S. Bielawski, D. Derozier, and P. Glorieux, Phys. Rev. A **46**, 2811 (1992).

[9] K. Otsuka, M. Georgiou, and P. Mandel, Jpn. J. Appl. Phys. **31**, L1250 (1992).

[10] N. M. Kroll, Phys. Rev. **127**, 1207 (1962).

[11] M. K. Oshman and S. E. Harris, IEEE J. Quantum Electron. **QE-4**, 491 (1968).

[12] T. Baer, J. Opt. Soc. Am. B **3**, 1175 (1986).

[13] G. E. James, E. M. Harrell II, and R. Roy, Phys. Rev. A **41**, 2778 (1990).

[14] M. Oka and S. Kubota, Opt. Lett. **13**, 805 (1988).

[15] G. E. James, E. M. Harrell II, C. Bracikowski, K. Wiesenfeld, and R. Roy, Opt. Lett. **15**, 1141 (1990).

[16] R. Roy, C. Bracikowski, and G. James, in *Proceedings of the International Conference on Quantum Optics,* edited by R. Inguva and G. S. Agarwal (Plenum, New York, in press).

[17] E. A. Victorov, I. B. Vitrishchak, G. E. Novikov, O. A. Orlov, A. A. Mak, V. A. Sokolov, V. I. Ustyugov, and M. M. Khaleev, in *Nonlinear Dynamics in Optical Systems,* edited by N. B. Abraham, E. Garmire, and P. Mandel, OSA Proceedings 7 (Optical Society of America, Washington, DC, 1991).

[18] E. A. Victorov, O. A. Orlov, A. A. Mak, and V. I. Ustyugov, SPIE Proc. Solid State Lasers, **1839**, 337 (1992).

[19] P. Mandel, M. Georgiou, K. Otsuka, and D. Pieroux, Opt. Commun. (to be published).